ANALES de Edificación

Received: 20/01/2025
Accepted:28/01/2025

Anales de Edificación
Vol. 11, Nº1, 1-8 (2025)
ISSN: 2444-1309
DOI: 10.20868/ade.2025.5504

Fabricación y comportamiento lumínico de la madera transparente
Manufacture and lightning performance of transparent wood

Belén Zapico Benavides[a]; Mercedes González Redondo[a]; Daphne Hermosilla Redondo[b]; Jose Ramón Aira Zunzunegui[a].

[a] Escuela Técnica Superior de Arquitectura. Universidad Politécnica de Madrid. b.zapico@alumnos.upm.es
[b] Escuela Técnica Superior de Ingeniería de Montes, Forestal y del Medio Natural, Universidad Politécnica de Madrid.

Resumen-- **La madera transparente se está empezando a utilizar en sustitución del vidrio en multitud de aplicaciones como, por ejemplo, en las pantallas de teléfonos móviles, en paneles solares o en las ventanas de edificios. Además de requerir menos energía para su obtención, la madera transparente tiene una conductividad térmica mucho menor que el vidrio. El objetivo de este trabajo consistió en explorar el proceso de fabricación de la madera transparente, así como en analizar los niveles de transparencia alcanzados mediante la medición del paso de la luz solar a su través (iluminancia). Para los ensayos se utilizaron tres especies de madera con distintas densidades: baja, media y alta. Se obtuvieron ecuaciones analíticas que permiten conocer la iluminancia a lo largo del día. Adicionalmente se estudió la influencia de la dirección de la fibra en relación con la trayectoria solar, descubriendo que la iluminancia aumenta cuando ambas son paralelas.**

Palabras clave— madera; transparente; fabricación; iluminancia.

Abstract— **Transparent wood is beginning to be used as a substitute for glass in a multitude of applications, such as in mobile phone screens, solar panels or building windows. In addition to requiring less energy to obtain, transparent wood has a much lower thermal conductivity than glass. The aim of this work was to explore the manufacturing process of transparent wood, as well as to analyse the levels of transparency achieved by measuring the passage of sunlight through it (illuminance). For the trials, three species of wood with different densities were used: low, medium and high. Analytical equations were obtained that allow us to know the illuminance throughout the day. Additionally, the influence of the direction of the fiber in relation to the solar path was studied, discovering that the illuminance increases when both are parallel.**

Index Terms— wood; transparent; manufacture; illuminance.

I. Introduction

THE continuous development of sustainable materials and eco-friendly processes is crucial for environmental conservation, as well as for responding to increasing energy scarcity. This principle forms the basis of this study.

The journey towards understanding and using transparent wood began with the study conducted at the KTH Royal Institute of Technology. This first research was fundamental to move from theory to practice, demonstrating the feasibility of transforming wood, a traditional and opaque material, into a transparent composite. The transformation was achieved through an initial delignification process of the wood and its subsequent infiltration with polymers such as methyl methacrylate (MMA), which gave the wood a remarkable transparency while preserving and even enhancing its structural integrity. The success of the KTH team laid the groundwork for further exploration of this novel material (Montanari et al., 2021).

On this basis, the University of Maryland played an important role in advancing the field. They delved into the

B.Z.B is PhD student at Escuela Técnica Superior de Arquitectura de Madrid, Universidad Politécnica de Madrid. M.G.R., and J.R.A.Z. are Associate professors at Escuela Técnica Superior de Arquitectura de Madrid.

D.H.R is associate professor at Escuela Técnica Superior de Ingeniería de Montes, Forestal y del Medio Natural, Universidad Politécnica de Madrid.

properties of transparent wood, revealing its potential to block UV rays, which is critical for applications in areas where protection from ultraviolet radiation is necessary. In addition, they conducted extensive studies on the mechanical strength of transparent wood, revealing that it not only maintains but can overcome natural resistance thanks to the contribution of the infiltrated polymer (Xia et al., 2021).

In addition, the environmental impact and biodegradability of transparent wood have been the subject of interest in numerous studies recently. All of them focus on its potential as an eco-friendly alternative, particularly as an alternative to conventional building materials such as plastic and glass. The biodegradability of transparent wood makes it a sustainable material, aligning with global efforts to reduce the environmental carbon footprint and promote eco-friendly materials in various industries(Jia et al., 2019; Gan et al., 2017, 2017; Zhu et al., 2016, 2016; Li et al., 2017, 2018, 2016; Qiu et al., 2019, Song et al., 2017, 2018; Vasileva et al., 2018; Li et al., 2019; Yu et al., 2017;Fink et al., 2009).

In conclusion, the journey from initial experiments at the KTH Royal Institute of Technology to extensive studies at the University of Maryland and other institutions marks a significant evolution in the realm of transparent wood development. The combined efforts of these research teams have not only revealed the fundamental physical properties of this material but have also opened avenues for its application in an innovative and environmentally sustainable way. As research continues, the potential uses and impacts of transparent wood in various sectors, particularly in the construction and design industries, will be expanded, paving the way for new architectures and technologies that use this unique material.

Transparent wood emerges as a remarkable innovation, challenging traditional materials such as glass and plastic with its unique set of properties.

Altering the microstructure of the wood allows light to disperse evenly, leading to consistent, softer lighting. This quality is particularly advantageous in architectural settings where taking advantage of natural light, without compromising privacy, is crucial. Transparency can be moderated depending on the thickness of the sample, for example, thinner pieces of wood have achieved up to 90% transparency, while thicker pieces have shown reduced, but significant, levels of transparency (Kanócz et al., 2020). Its ability to guide sunlight through its fibers optimizes natural light regardless of the position of the sun. This property results in a very uniform and soft distribution of light within the interior spaces, which, not only improves aesthetics and comfort, but also reduces the need for artificial lighting during the day and therefore energy. Such a feature is particularly valuable in latitudes where the position of the sun varies significantly throughout the year, ensuring that indoor spaces receive optimal and consistent lighting regardless of the season (Xia et al., 2021).

In addition to its optical properties, transparent wood also has greater mechanical resistance. The substitution of lignin, which is a component of wood distributed mainly in the secondary cell wall and provides rigidity to the cell walls with polymeric materials, not only maintains, but can improve the strength and rigidity of the whole, making it an attractive alternative for various structural applications (Kanócz et al., 2020; Katunský et al., 2018).

However, one of the most striking characteristics of this material is its low thermal conductivity. By maintaining the original structure, filling the spaces left by the lignin with polymeric materials that have low thermal conductivity, transparent wood also acquires this insulating capacity. This means that in addition to integrating into designs naturally, it keeps heat constantly inside, thus reducing the need for heating and cooling systems. It is an environmentally sustainable as well as energy-efficient solution (Jele et al., 2023; Chen et al., 2020).

The aim is to explore the manufacturing process of transparent wood, with a particular focus on its translucency properties for different types of wood and manufacturing methods. The aim is to understand and optimize the chemical and physical processes involved in its production, for its subsequent use in construction.

II. Research methodology

A. *Transparent wood manufacturing in the laboratory*

The manufacture of transparent wood consists of two main steps: the delignification of the wood, in which the lignin is removed, and the infiltration of a transparent polymer. The variants in the studies are the chemicals used in the delignification process and the type of polymer.

The epoxy resin infiltration method has recently been used by some researchers (Jia et al., 2019), who managed to manufacture transparent wood after delignification of natural balsa wood using sodium chlorite ($NaClO_2$), followed by infiltration with epoxy resin. They achieved a high transmittance of 79.4%, but with high haze (or turbidity).

The KTH Royal Institute of Technology study uses another method, that of infiltration with methyl methacrylate (PMMA), a thermoplastic polymer. Balsa wood was also used by delignifying it with sodium chlorite. This technique produced transparent wood with 90% transmittance and very low haze (10%) at a thickness of 0.7 mm (Montanari et al., 2021).

Instead of PMMA, Zhu (2016) used AeroMarine Epoxy #300/21. They first removed lignin with sodium hydroxide (NaOH), sodium sulfite (Na_2SO_3), and hydrogen peroxide.

In the development of this work, wood specimens of low thickness (2 millimeters) have been selected, because these dimensions facilitate a more efficient and practical handling during the experimental process. For the crucial stage of delignification, the use of sodium chlorite has been chosen. This choice is based on its high efficiency in delignifying the wood, allowing a high content of voids that allow the subsequent inclusion of a polymer. Regarding the infiltration process, it has been decided to use epoxy resin for its capacity for infiltration and transparency.

Thus, the materials used for the production of the specimens were the following (Fig. 1):

- Wood types: balsa (density: 125 kg/m³), maple

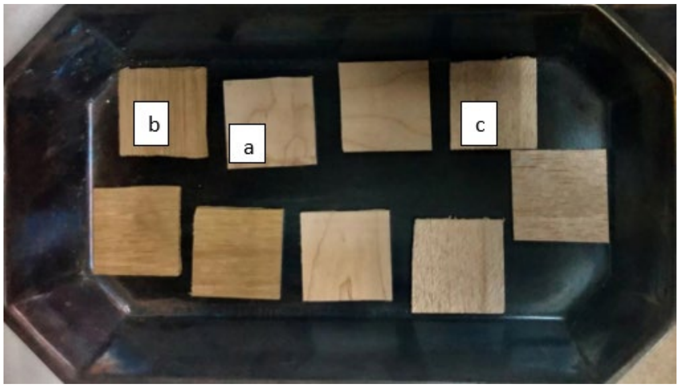

Fig. 1. Balsa (b), maple (a) and oak (c) specimens. (Source: authors)

(density: 570 kg/m³) and oak (density: 735 kg/m³). Specimens of 40x40x2 mm.

The chemical products used have been the following:

- Sodium Acetate Trihydrate: 1.67 g
- Acetic acid: Initially 1.15 ml, variations up to 2.5 ml.
- Sodium chlorite: 1.3 g.
- Distilled water: 125 ml.
- Ethanol, acetone, and epoxy resin in specific amounts.

In order to study the importance of wood density in the process, three types of wood were used: balsa wood with a low density of 125 kg/m3, maple wood with an average density of 570 kg/m3 and oak wood with a high density of 735 kg/m3.

The pieces were cut into small squares of 4 by 4 cm (2 mm thick) and placed in the oven for 24 hours at 105°C so that the remaining water inside evaporated and thus the chemical modification of the structure of the material could proceed. An acetate buffer solution was used to keep the pH of the reaction stable and to be able to adequately control the delignification reactions with 1% sodium chlorite by weight and acetic acid that allow the subsequent incorporation of the polymer. Lignin is an organic polymer rich in aromatic structures that can be degraded by chlorine dioxide that is formed in the reaction of sodium chlorite with an acid such as acetic acid. Wood acetylation promotes polymer compatibility with the delignified cell wall of wood (Li et al., 2018).

The wood was treated at 80ºC. When this temperature was reached in the previously prepared solution, the balsa wood piece was introduced for your treatment and allowed to react for 24 hours.

The wood reacted with the solution, degrading the lignin molecules and their chromophore groups, so that the wood acquired a whitish and translucent tone (Fig. 2). Variations in formulation were studied to see the increase in lignin degradation and thus the subsequent transparency of the wood. Different concentrations of glacial acetic acid from 1.15 mL to 2 mL, 2.25 mL, and 2.5 mL were tested in 150 mL of solution; and the results were compared in 3 different solutions, keeping the rest of the variables the same (Fig. 3). The doubling of the concentration of all the reagents was also studied.

The production of chlorine dioxide in the presence of acetyl groups produces the controlled delignification of the material, affecting the lignin chromophore groups that decrease the transparency and whiteness of the wood. The presence of acetyl groups produces the acetylation of part of the material, allowing greater compatibility of the polymer with the delignified cell wall. As can be seen in the following reactions, the oxidation of lignin results in the formation of lignin fragments, some of which are soluble in water. This can be seen in phenolic hydroxyl groups, which are part of lignin, where after oxidation, it is converted to phenolic oxide. Lignin also contains ether bonds, particularly β-O-4 bonds, which are common in its structure. Chlorine dioxide can break these bonds, leading to the formation of smaller fragments.

The increase in the concentration of reagents did not improve the transparency of the material, so to improve delignification, the number of treatments was increased while maintaining the initial proportions of the reagents.

It was visually verified that, after a single treatment, the wood did not have enough whiteness, so the repetition of 2, 3, 4, 8 and 10 treatments was tested, demonstrating that as the number of treatments increased, more lignin was eliminated, evidenced by obtaining a whiter color and a greater number of pores in the material and, therefore, increasing the transparency of the wood (Figures 4 and 5).

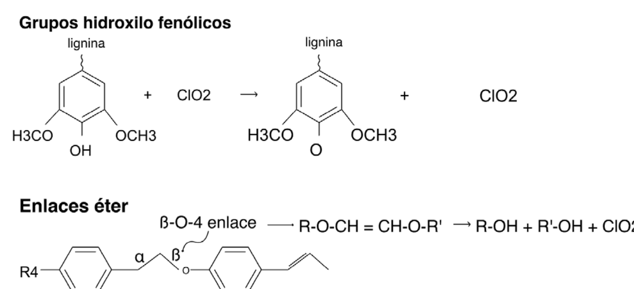

The next step was to clean the wood of any residue from the solution. The cleaning was carried out by immersing the pieces first in distilled water and then in ethanol and acetone for 12 hours each. This process eliminated any remaining reagents used in the treatment and residues produced during the treatment that may have remained inside the wood. After

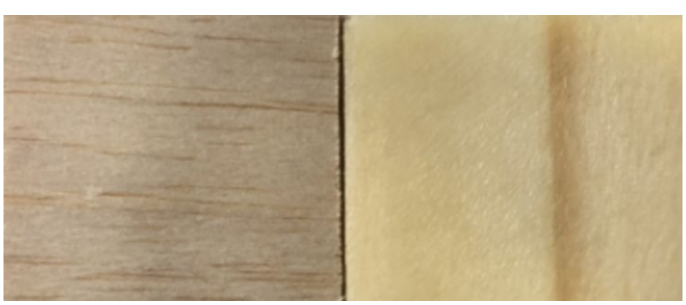

Fig. 2. Untreated balsa wood (left) and treated (right). (Source: authors)

Fig. 3. Wooden specimens with different solutions. (Source: authors)

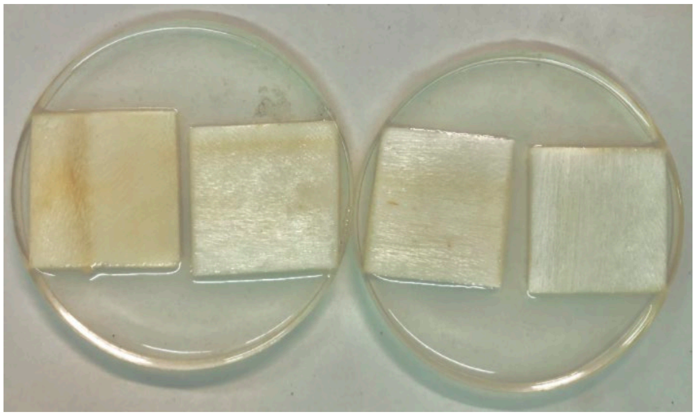

Fig. 4. Balsa wood after the application of 1, 2, 4 and 6 treatments (left to right). (Source: authors)

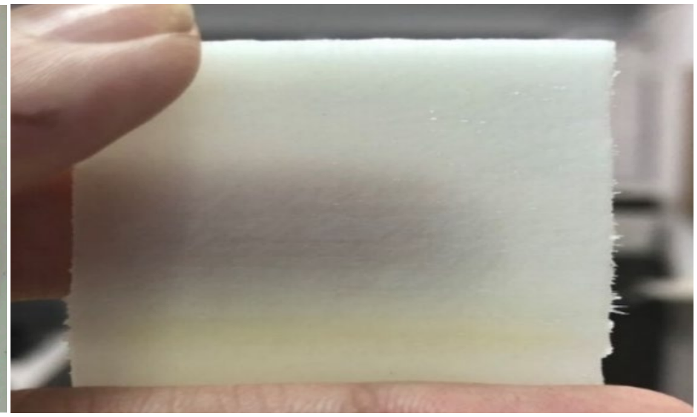

Fig. 5. Balsa wood with 6 treatments before resin infiltration. (Source: authors)

cleaning, the wood samples were still not transparent due to light scattering at the interface between the cell wall and the air.

The pores of the wood must be filled with a polymeric material that has a refractive index similar to the transparent wood itself to recover the rigidity lost by delignification and, in turn, improve the transparency of the product. To do this, transparent epoxy resin was used, which has a refractive index (IR) of 1.565 ± 0.0005, which is very similar to that of glass (IR= 1.480). The wood was placed in the resin inside the vacuum chamber to remove the air inside the plant cells so that they could later be filled with resin, Fig. 6. The appearance of bubbles on the outside of the specimens indicated that air bubbles were being removed from the inside of the wood, Fig. 7.

The process shown had been carried out with balsa wood. The next step was to try to achieve the same transparency with the other two types of wood: maple and oak. The same procedures were applied for both, trying to apply the same number of treatments (1, 2, 3, 4, 8 and 10), however, after the infiltration of the epoxy resin it could be verified, both at a macroscopic and microscopic level, that balsa wood had much more transparency than any of the other wood species. probably due to its lower density, which facilitates its delignification, and indicates a greater number of pores in it, which treated and infiltrated with resin increases its transparency, figures 8 and 9. Maple and oak woods were therefore discarded for the next phase.

B. Lighting study

In this second phase of the work, the effectiveness of transparent wood previously manufactured in the laboratory was analysed from a lighting point of view. Specifically, the research focused on the ability of transparent wood to transmit

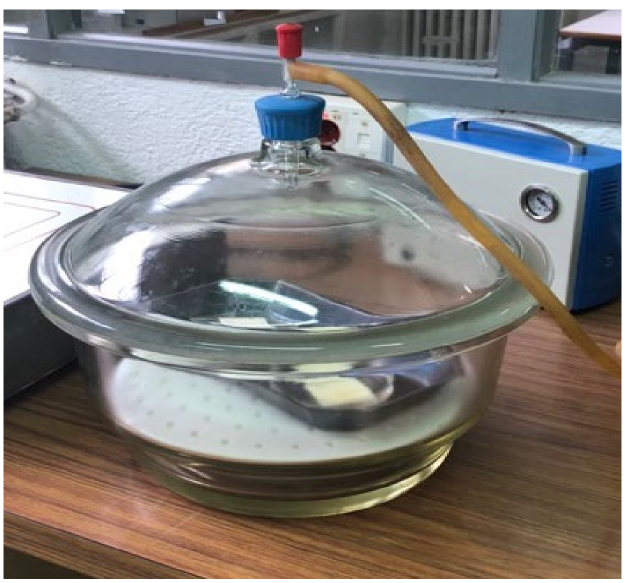

Fig. 6: Vacuum hood for epoxy resin primer. (Source: authors)

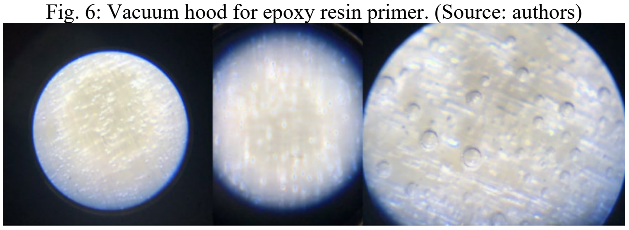

Fig. 7: Air bubbles coming from inside the specimen.

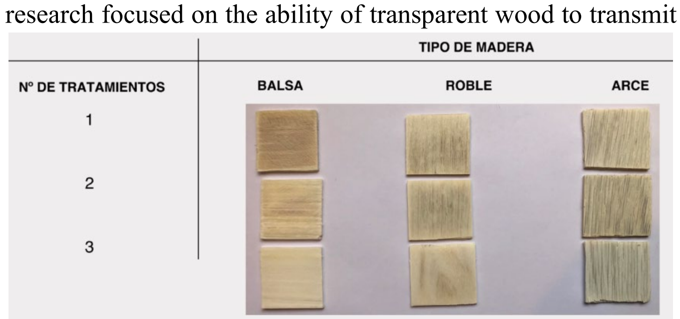

Fig. 8: Comparison of the whiteness achieved in balsa, maple and oak specimens with 1, 2 and 3 treatments. (Source: authors)

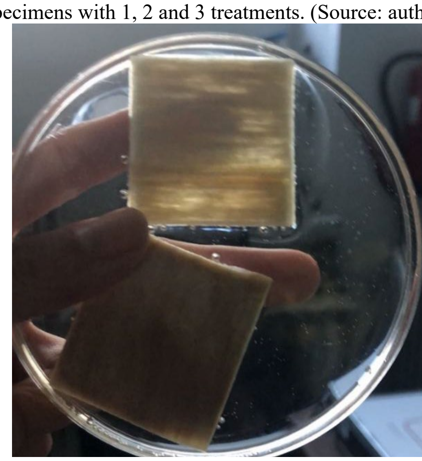

Fig. 9: Balsa wood (top) and maple wood (bottom) with 4 treatments after resin infiltration. (Source: authors)

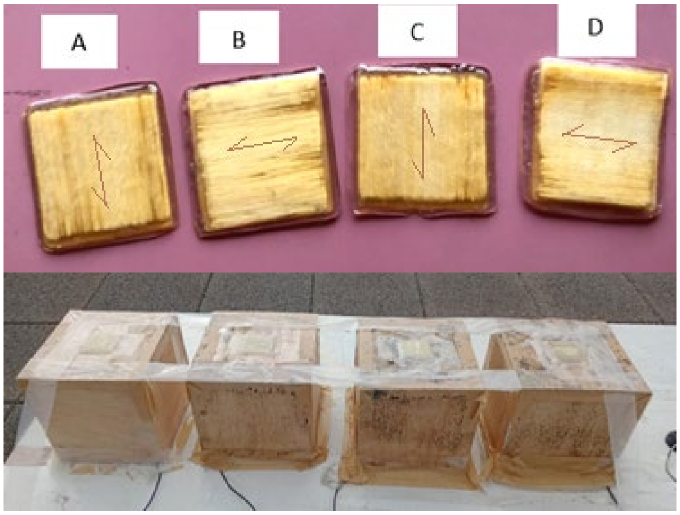

Fig. 10: Specimens A, B, C, and D placed on the top of their corresponding models. The direction of the wood fiber (top) is seen in relation to the direction of the solar path (bottom). (Source: authors)

light in two different situations: with the direction of the wood fibre parallel to the direction of the solar path, and with the direction of the fibre perpendicular to the direction of the solar path.

To do this, an experiment was designed that consisted of the construction of four models, simulating four small houses, which would serve as test chambers, Fig. 10. A hole was opened in the upper part of each model, as a window, over which the corresponding transparent wooden test tube was placed. The models were built using opaque wooden boards with dimensions of 20 x 20 cm to obtain a cube of 20 cm on a side. The upper hole had dimensions of 4 x 4 cm.

For the study, four balsa wood specimens were manufactured, all of them subjected to ten different treatments. Specimens A and B exhibited a transparency level of 75%, which means that 75% of their surface is transparent and the remaining 25% is opaque. Similarly, specimens C and D had a transparency level of 50%.

Additionally, to study the influence of the fiber direction on the interior illuminance, the models were placed in such a way that specimens A and C had the direction of the fiber perpendicular to the direction of the solar path, while specimens B and D had the direction of the fiber parallel to the solar path.

Photometric sensors placed in the geometric center of its base were used to measure the illuminance inside each model, coinciding exactly with the location of the wooden specimens

Fig. 12: Li-210 photometric sensor (left) and datalogger (right). (Source: authors)

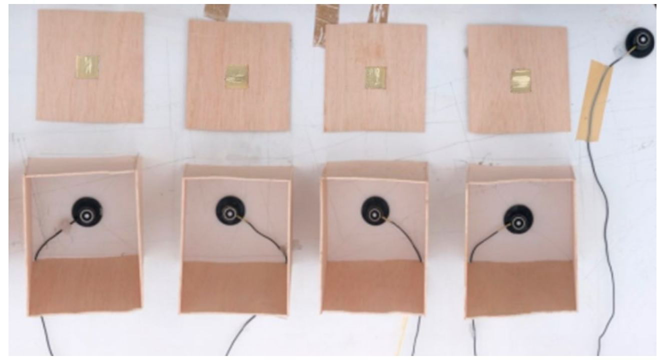

Fig. 11: Placement of the sensors inside the models. (Source: authors)

on the upper face, Fig. 11. All models were carefully sealed using brown tape. This sealing ensured that no external light entered the models so that it would not interfere with the reading of the sensors. The experiment was scheduled to take place over five sunny days, from February 01 to 05, 2024, during which the sensors would record continuously (LICOR, 1987).

The experiment was physically carried out on the flat roof of the Higher Technical School of Architecture, a place totally free of shadows, thus providing a realistic and controlled environment for the rehearsals.

For this study, analog photometric sensors, model LI-210 PHOTOMETRIC, of the LI-COR brand, connected to the channels of a Li-1000 datalogger by means of a board and two 6 BNC connectors, Fig. 12, were used. Previously, the sensors were calibrated, obtaining the calibration constants shown in Table 1.

The datalogger was set to record measurements every 5 minutes for the five days, as long as they were greater than 1 lux, so the graphs all start at sunrise and end at sunset.

To download the data, the datalogger was connected to the computer via a 25-pin cable and the LICOR COMM program, compatible with Excel, was used. In Excel, this data appears in rows separated by days, times, and the name of the photometric sensor. These values are given in kiloluxes (Klx). With the recorded data, graphs were created that relate the illuminance to the time of day.

III. Results

A. *Transparency*

Fig. 13 shows that the wood resulting from the infiltration of the resin exhibits significant variability in transparency levels. The edge of the sample has a level of total transparency because it is the leftover resin that borders the wooden specimen. The edges of the wood then show a high level of transparency,

Table I
Calibration constants of the sensors

Sensor	Channel	Model	Calibration Constant	Direction of the fibres with respect to the solar path
6	1	A	3,7004	perpendicular
4731	2	B	3,1161	parallel
5780	3	C	3,1951	perpendicular
4707	4	D	3,4175	parallel
5784	6	OUTSIDE	4,1225	---

Fig. 13: Balsa wood after 10 treatments and subsequent impregnation with epoxy resin. (Source: authors)

suggesting an effective infiltration of the resin in this area. A medium level of transparency is then identified, characterized by a darker tone, indicating that the resin has partially penetrated the wood. Finally, inside the sample, a low level of transparency stands out, represented by a whitish tone. On the other hand, in the area of low transparency level, the direction of the fiber and how the transparency between some fibers is greater to form slits through which light can pass through.

The difference in transparency between the edges and the center of the wood could indicate that the resin was not able to fully penetrate the interior of the material. This phenomenon could be attributed to the type of resin used which, despite the density being similar to that of water (1,141 g/cm3), had higher viscosity, which could have influenced its impregnation capacity. Another possibility is that the pressure applied during the process was not high enough.

On the other hand, the lack of total transparency in the areas where the resin penetrated may be due to the fact that the refractive index of the resin was not sufficiently similar to that of wood. Some researchers recommend an index of about 1.5 (Mi et al., 2020).

B. *Illuminance*

After several days of data collection, a series of results were obtained that shed light on the effectiveness of different materials in transmitting light. Of the five days of continuous measurement, the data corresponding to two of them (February 2 and February 3) were chosen because they were sunny days with low cloud cover that gave rise to more homogeneous data.

With the information from the four models and from the outside, a series of graphs were made that relate the illuminance, on the axis of ordinates, with the time of day, on the axis of abscissae, figures 14 and 15. Through these graphs it is possible to know the light that enters the interior of each model, as well as the light outside. The exterior illuminance is much higher than that of the models, so it was necessary to present two graphs, one including the exterior sensor with the rest, and another without including it in order to compare the models with each other.

Fig. 14 shows perfectly how the sensors have an adequate sensitivity to the parameter to be recorded. Thus, it is observed that at 3:45 p.m. the presence of a cloud generates a shadow that reduces the illuminance both on the outside of the models and on the inside.

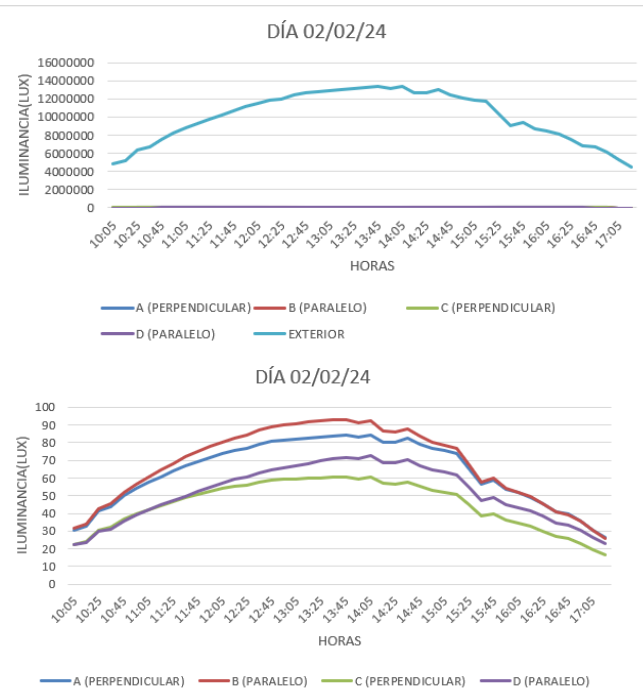

Fig. 14: Illuminance graphs of February 2, 2024. Models with exterior (top), and models without exterior (bottom). (Source: authors)

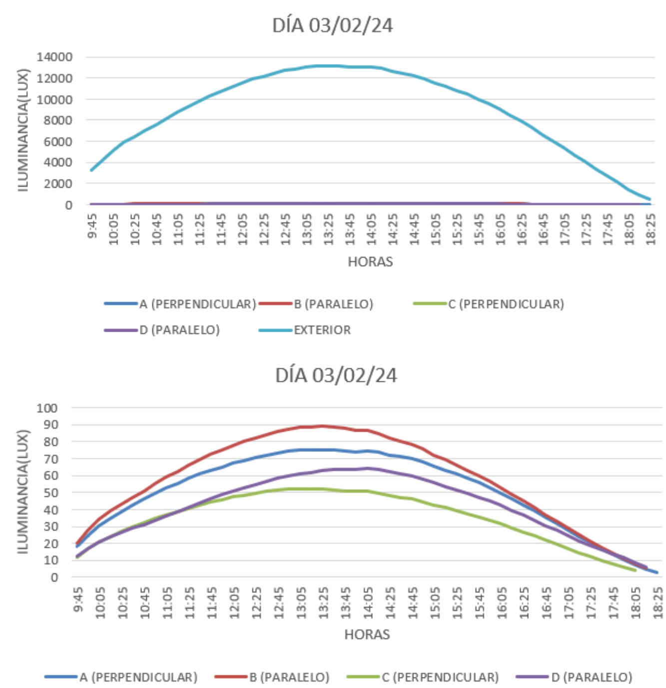

Fig. 15: Illuminance graphs of February 03, 2024. Models with exterior (top), and models without exterior (bottom). (Source: authors)

The graphs in Figures 14 and 15 clearly show that models A and B, with a transparency of 75%, have significantly higher illuminance than specimens C and D, with a transparency of 50%. This finding is consistent with the theory since, the greater the transparency, the greater the amount of light that is able to enter the interior of the models.

Additionally, the influence of the direction of the wood fibers on the results is highlighted. Models B and D, with fibers arranged parallel to the path of the sun, exhibit a clearly superior illuminance compared to models A and C, whose fibers are arranged perpendicularly. This phenomenon underlines the relevance of the orientation of the fibers in the ability of wood to allow light to pass through, confirming that the parallel direction significantly maximizes light transmission.

Finally, taking advantage of the fact that the curves of February 3 exhibit a remarkable uniformity, Fig. 15, a simple regression analysis was carried out to obtain analytical equations that relate the illuminance, inside each model, with the time on a sunny day. Second-degree polynomial equations were obtained with coefficients of determination close to unity ($R^2 \approx 0.98$), indicating an excellent correspondence between the observed data and the predicted values.

TABLE II
ANALYTICAL EQUATIONS TO DETERMINE ILLUMINANCE AS A FUNCTION OF TIME OF DAY

Model	Analytic equation	R^2
A	I = -1970.1t2 + 2228.6t – 556.67	0,9867
B	I = -2321.9t2 + 2614.6t – 651.84	0,9789
C	I = -1456.8t2 + 1638.6t + 409.93	0,9852
D	I = -1681.7t2 + 1925.4t – 490.76	0,9812

IV. CONCLUSIONS

Throughout this study, it has been possible to organize and complete the entire process related to the manufacture of transparent wood and the subsequent analysis of the corresponding lighting.

The test material consisted of three wood species with different densities: low-density balsa wood, medium-density maple wood, and high-density oak wood.

In relation to transparency, the process of manufacturing transparent wood in the laboratory was effective only with balsa wood, verifying that by increasing the number of treatments, more lignin was removed and, with this, it was possible to achieve greater transparency.

In relation to illuminance, a clear relationship was observed between the illuminance and the transparency of the specimens so that, the greater the transparency, the greater the ability to transmit light through them and, therefore, the greater the illuminance. In addition, analytical equations were obtained that allow us to know the illuminance throughout the day. Additionally, the influence of the direction of the wood fiber was studied, discovering that the illuminance increases when the direction of the fiber is parallel to the direction of the solar path.

The document has clearly identified the potential challenges and improvements needed to optimize results in future research.

ACKNOWLEDGEMENTS

The authors would like to thank Luis de Villanueva Construction Materials Laboratory and the Higher Technical School of Architecture of the Polytechnic University of Madrid for providing their facilities for the development of this research.

REFERENCES

C. Montanari, Y. Ogawa, P. Olsén, L.A. Berglund. 2021. *High Performance, Fully Bio-Based, and Optically Transparent Wood Biocomposites*. Advanced science, volume 8 issue 12, 2198-3844. DOI: 10.1002/advs.202100559

Q. Xia, C. Chen, T. Li, S. He, J. Gao, X. Wang, L. Hu. 2021. *Solar-assisted fabrication of large-scale, patternable transparent wood*. Science Advances, volume 7 number 5. DOI: 10.1126/sciadv.abd7342

C. Jia, C. Chen, R. Mi, T. Li, J. Dai, Z. Yang, Y. Pei, S. He, H. Bian, S.H. Jang, J.Y. Zhu, B. Yang, L. Hu. 2019. *Clear wood toward high-performance building materials*. ACS nano, 13, 9993-10001 pp. DOI: 10.1021/acsnano.9b00089

W. Gan et al. 2017. *Luminescent and Transparent Wood Composites Fabricated by Poly(methyl methacrylate) and γ-Fe2O3@YVO4:Eu3+ Nanoparticle Impregnation*. ACS Sustainable Chemistry & Engineering, 5, 3855-3862.

W. Gan, L. Gao, S. Xiao, W. Zhang, X. Zhan, J. Li. 2017. *Transparent Magnetic Wood Composites Based on Immobilizing Fe3O4 Nanoparticles into a Delignified Wood Template*. Journal of Materials Science, 52, 3321-3329. DOI: 10.1007/s10853-016-0619-8

M. Zhu, J. Song, T. Li, A. Gong, Y. Wang, J. Dai, Y. Yao, W. Luo, D. Henderson, L. Hu. 2016. *Highly Anisotropic, Highly Transparent Wood Composites*. Advanced Materials, 28, 5181-5187. DOI: 10.1002/adma.201600427

T. L, M. Zhu, Z. Yang, J. Song, J. Dai, Y. Yao, W. Luo, G. Pastel, B. Yang, L. Hu. 2016. *Wood Composite as an Energy Efficient Building Material: Guided Sunlight Transmittance and Effective Thermal Insulation*. Advanced Energy Materials, 6, 1601122. DOI: 10.1002/aenm.20160122

Y. Li, S. Yu, J.G.C. Veinot, J. Linnros, L. Berglund, I. Sychugov. 2017. *Luminescent Transparent Wood*. Advanced Optical Materials, 5, 1600834. DOI: 10.1002/adom.201600834

Y. Li, X. Yang, Q. Fu, R. Rojas, M. Yan, L. Berglund. 2018. *Towards Centimeter Thick Transparent Wood through Interface Manipulation*. Journal of Materials Chemistry A, 6, 1094-1101. DOI: 10.1039/c7ta09973h

Y. Li, Q. Fu, S. Yu, M. Yan, L. Berglund. 2016. *Optically Transparent Wood from a Nanoporous Cellulosic Template: Combining Functional and Structural Performance*. Biomacromolecules, 17, 1358-1364. DOI: 10.1021/acs.biomac.6b00145

Z. Qiu, Z. Xiao, L. Gao, J. Li, H. Wang, Y. Wang, Y. Xie . 2019. *Transparent Wood Bearing a Shielding Effect to Infrared Heat and Ultraviolet via Incorporation of Modified Antimony-Doped Tin Oxide Nanoparticles*. Composites

Science and Technology, 172, 43-48. DOI: 10.1016/j.compscitech.2019.01.005

J. Song, C. Chen, Z. Yang, Y. Kuang, T. Li, Y. Li, H. Huang, I. Kierzewski, B. Liu, S. He, T. Gao, S.U. Yuruker, A. Gong, B. Yang, L. Hu. 2018. *Highly Compressible Anisotropic Aerogel with Aligned Cellulose Nanofibers*. ACS Nano, 12, 140-147. DOI: 10.1021/acsnano.7b04246

E. Vasileva, H. Chen, Y. Li, I. Sychugov, M. Yan, L. Berglund, S. Popov. 2017. *Light Scattering by Structurally Anisotropic Media: A Benchmark with Transparent Wood*. Advanced Optical Materials, 6, 1800999.DOI:10.1002/adom.201800999

T. Li, S.X. Li, W. Kong, C. Chen, E. Hitz, C. Jia, J. Dai, X. Zhang, R. Briber, L. Hu. 2019. *A nanofluidic ion regulation membrane with aligned cellulose nanofibers*. Science Advances, 5, eaau4238. DOI: 10.1126/sciadv.aau4238

Z. Yu, Y. Yao, J. Yao, L. Zhang, Z. Chen, Y. Gao, H. Lou. 2017. *Transparent Wood Containing Cs0.33WO3 Nanoparticles for Heat-Shielding Window Applications*. Journal of Materials Chemistry A, 5, 6019-6024. DOI:10.1039/C7TA00261K

J. Song, C. Chen, C. Wang, Y. Kuang, Y. Li, F. Jiang, Y. Li, E. Hitz, Y. Zhang, B. Liu, A. Gong, H. Bian, J.Y. Zhu, J. Zhang, J. Li, L. Hu 2017. *Superflexible Wood*. ACS Applied Materials & Interfaces, 9, 23520-23527. DOI: 10.1021/acsami.7b06529

S. Fink. 2009. *Transparent Wood – A New Approach in the Functional Study of Wood Structure Holzforschung*. International Journal of the Biology, Chemistry, Physics and Technology of Wood, 46, 403-408. DOI: 10.1515/hfsg.1992.46.5.403

J. Kanócz, V. Bajzecerová, V. Karl´a. 2020. *Analysis of mechanical properties of I-beam with web from transparent wood*. IOP Conf. Ser. Mater. Sci. Eng. 867 012017. DOI:10.1088/1757-899X/867/1/012017

D. Katunský, J. Kanócz, V. Karľa. 2018. *Structural Elements with Transparent Wood in Architecture*. International Review of Applied Sciences and Engineering (IRASE), 2, 101-106. DOI:10.1556/1848.2018.9.2.4

T.B. Jele, J. Andrew, M. John, B. Sithole. 2023. *Engineered transparent wood composites: a review*. Cellulose 30, 5447–5471. DOI:10.1007/s10570-023-05239-z

R. Mi, C. Chen, T. Keplinge, Y. Pei, S. He, D. Liu, J. Li, J. Dai, E. Hitz, B. Yang, I. Burgert, L. Hu. 2020. *Scalable aesthetic transparent wood for energy efficient buildings*. Nat Commun 11, 3836. DOI:10.1038/s41467-020-17513-w

Y. Li, E. Vasileva, I. Sychugov, S. Popov, L. Berglund 2019. Optically Transparent Wood: Recent Progress, Opportunities, and Challenges Adv. Optical Mater 6, 1800059. DOI:10.1002/adom.201800059.

LICOR. LI-1000 DataLogger, Instruction Manual. Lincoln: Nebraska, revision 1: November, 1987; 157 páginas.

LICOR. LI 210SA Photometric sensor, Specifications. Lincoln: Nebraska.